2004

Thermal and Fluid Dynamic Behavior of Trans-Critical Carbon Dioxide Hermetic Reciprocating Compressors: Numerical Analysis

Carlos D. PerÃ©z Segarra
Universitat Politècnica de Catalunya

Joaquim Rigola
Universitat Politècnica de Catalunya

Assensi Oliva
Universitat Politècnica de Catalunya

THERMAL AND FLUID DYNAMIC BEHAVIOR OF TRANS-CRITICAL CARBON DIOXIDE HERMETIC RECIPROCATING COMPRESSORS: NUMERICAL ANALYSIS

Carlos D. PEREZ-SEGARRA, Joaquim RIGOLA, Assensi OLIVA

Centre Tecnològic de Transferència de Calor CTTC,
Laboratori de Termotècnia i Energètica,
Dept. Màquines i Motors Tèrmics. Universitat Politècnica de Catalunya,
Colom 11, 08222 Terrassa (Barcelona), Spain
Fax: +34-93-739.89.20, Tel. +34-93-739.81.92
E-mail: labtie@labtie.mmt.upc.es, Web page: http://www.cttc.upc.edu

ABSTRACT

The objective of this work is to define the main geometrical characteristics of a hermetic reciprocating compressor working with CO_2 under trans-critical conditions. The working conditions considered are: a refrigerating capacity of 800 W, an evaporation temperature of 7.2^oC and a super-heating temperature of 35^oC, with a gas cooler temperature of 46^oC. Firstly, a brief presentation of the refrigerating cycle based on pure thermodynamic analysis is presented, with the idea to analyse the differences between a conventional sub-critical R134a cycle and a trans-critical CO_2 cycle. After the thermodynamic analysis, a numerical comparative study of both compressor models is presented for the same conditions. The present paper finishes with a CO_2 prototype compressor description, experimentally tested in a companion paper.

1. INTRODUCTION

According to the last Montreal and Kyoto protocols ((UNEP), 1987) ((UNFCCC), 1997), and their consequences, the domestic and commercial refrigeration, together with heat pump industries, are in a process of evaluation and introduction of new non-contaminant and natural refrigerants to replace HCFCs and HFCs, with the aim to use a refrigerant with nul Ozone Depletion Potential (ODP) and Global Warming Potential (GWP). The substitution of CFCs or HCFCs by HFCs or hydrocarbons and mixtures, presents less problems, because thermo-physical properties and work ranges are very similar. The introduction of natural refrigerants like CO_2 involves more complex problems (Lorentzen and Pettersen, 1993),(Lorentzen, 1994),(Jakobsen, 1998),(Kruse et al., 1999), (Kruse et al., 1999),(Pearson, 2001),(Taylor, 2002) and (Fleming, 2003). Each component and the whole refrigeration system have to be studied, modeled, developed and improved to assess a successful and guaranteed application, taking into account the highest work pressures, the heat exchangers dimensions and the compressor performance.

The first thermodynamic question is how to determine the gas cooler pressure in a trans-critical cycle, where there is no saturation temperature during the cooler gas phenomena (Liao et al., 2000),(Rozhentsev and Wang, 2001). The second aspect treated is a numerical comparative study between a conventional R134a compressor of $9cm^3$ and a new carbon dioxide prototype of $1.5cm^3$. The results have been obtained by means of a complete and advanced numerical simulation model of the thermal and fluid-dynamic performance of hermetic reciprocating compressors developed to be used in the whole domain (Pérez-Segarra et al., 2003). The quality of the numerical solution has been extensively verified, while the experimental validation of the numerical model has been carried out under a wide range of working conditions, compressor geometries and refrigerant fluids (Rigola et al., 2003), before adapting the numerical code to be used considering carbon dioxide properties. In this case, the comparative analysis show promising expectations.

The studied cases show the differences between the simplified thermodynamic analysis and the numerical simulation model results, which present better promising perspectives, and a CO_2 compressor prototype closer to a conventional compressors performance. The compressor prototype development, and its testing in an experimental trans-critical carbon dioxide unit, is presented in a companion paper (Rigola et al., 2004).

2. THERMODYNAMIC ANALYSIS

The working conditions of a conventional sub-critical system working with synthetic refrigerants can be defined by the following parameters usually given as design conditions for single-stage system, detailed in Figure 1 and depicted in Figure 1: evaporation temperature (T_{ev}), condensation temperature (T_c), superheating temperature (T_{sh}=T_1), sub-cooling temperature (T_{sc}=T_3).

Table 1: Sub-critical R134a cycle.

T_{ev}	p_{ev}	T_{sc}	p_c	T_c	T_{sh}	T_{amb}
T_4	p_4, p_1	T_3	p_3, p_2		T_1	
[^{o}C]	[bar]	[^{o}C]	[bar]	[^{o}C]	[^{o}C]	[^{o}C]
7.2	3.77	46	14.92	55.0	35.0	35.0

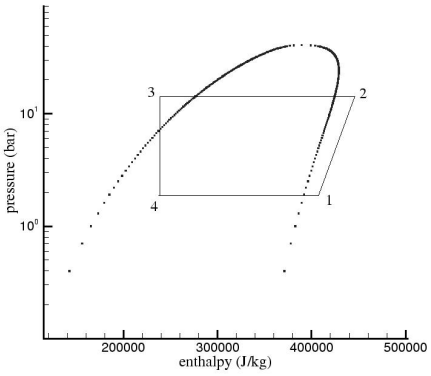

Figure 1: Pressure enthalpy R134a diagram.

It is well known that, for these conventional sub-critical systems, the Coefficient of Performance (COP) increases when the condensation temperature decreases, and consequently its saturation pressure. The reason for this behavior is that the pressure ratio decreases, and consequently the compressor work also decreases, while the refrigerating production is kept almost unchanged.

For a trans-critical carbon dioxide cycle working under the single-stage system, the design cycle conditions usually defined are detailed in Table 2 and depicted in Figure 2 as follows: evaporation temperature (T_{ev}), gas cooler pressure (p_{gc}), superheating temperature (T_{sh}=T_1) and gas cooler outlet temperature (T_3).

Table 2: Trans-critical CO_2 cycle.

T_{ev}	p_{ev}	T_{gc}	p_{gc}	T_{sh}	T_{amb}
T_4	p_4, p_1	T_3	p_3, p_2	T_1	
[^{o}C]	[bar]	[^{o}C]	[bar]	[^{o}C]	[^{o}C]
7.2	41.93	46	—	35.0	35.0

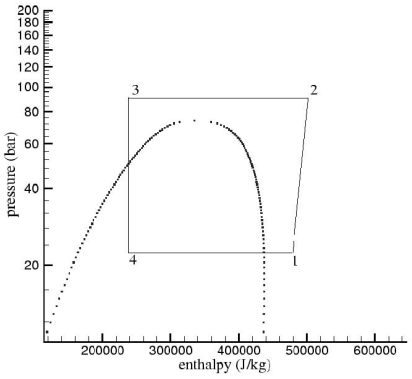

Figure 2: Pressure enthalpy CO_2 diagram.

The selection of the gas-cooler pressure is not clear. In fact, there is no evidence that lower gas-cooler pressure means higher COP, as in conventional sub-critical systems.

Figure 3 shows a thermodynamic comparative study of both sub-critical and trans-critical cycles, under ideal working conditions (isentropic compression, no heat or pressure losses, etc.). The Figures show the cooling capacity evolution, the specific compression work and the COP for different condenser (sub-critical) or gas cooler (trans-critical) pressures.

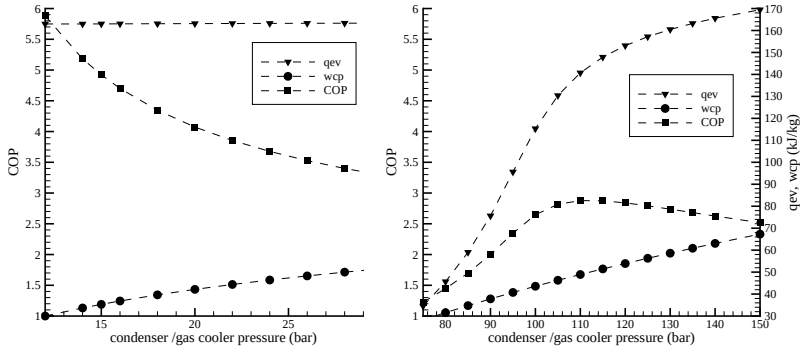

Figure 3: Heat, work and COP evolution; left: R134a; right: CO_2.

The results of the sub-critical cycle show that COP drastically decreases when condenser pressure increases. For the same conditions, compression work increases, while the evaporator heat is almost constant. Thus, R134a conditions depend only on the condenser temperature desired.

The same results of the trans-critical cycle shows that COP increases rapidly until a maximum point and then slowly decreases, when gas cooler pressure increases. The compression work always increases linearly with a unique slope, while the evaporator heat always increases, although with different slopes depending on gas cooler pressure, when gas cooler pressure increases. Thus, CO_2 conditions have an optimum gas cooler pressure for a maximum COP. In the conditions proposed, the optimum gas cooler pressure is between 100 and 110 bars.

Consequently, the influence of the optimum gas cooler pressure point depending on the evaporation temperature must be given. Figure 4 shows the same results presented above (Figure 3) under different evaporation temperatures.

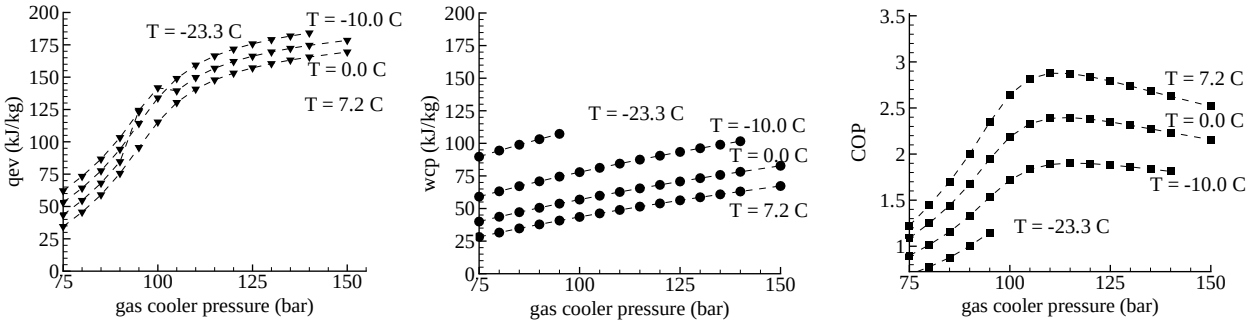

Figure 4: Specific evaporation heat, specific work and COP under CO_2 trans-critical cycle, for different evaporation temperatures.

The results in Figure 4 show that the three parameters (q_{ev}. w_{cp} and COP) present a very similar evolution. It is possible to observe that in all cases, and independently of the evaporation temperature, the optimum and maximum COP point is almost the same.

3. NUMERICAL COMPARATIVE ANALYSIS

A commercial hermetic reciprocating compressor GLY80 (of CUBIGEL, S.A.), working with R134a under the conventional sub-critical cycle of Table 1 for a cooling capacity around 700 kcal/h, is numerically compared with a CO_2 compressor prototype (called CL15) under the trans-critical cycle of Table 2 for a similar cooling capacity. The objective is to numerically compare the two compressor models under similar situations and comparative cooling capacities (i.e. working conditions).

3.1 Numerical simulation model

A detailed numerical simulation of the thermal and fluid dynamic behavior of reciprocating compressors commonly used in household refrigerators and freezers has been developed (Pérez-Segarra et al., 2003). The quality of the numerical solution has been verified by means of a critical analysis of the different numerical sources of errors: convergence errors, discretization errors, programming errors, etc. The accuracy of the mathematical model developed (modeling errors) has been obtained in an accurate and extensive experimental validation (Rigola et al., 2003) of different compressor geometries tested considering a wide range of working conditions and refrigerant fluids.

The model is based on the integration of the transient fluid conservation equations (continuity, momentum and energy) in the whole compressor domain (compression chamber, valves, manifolds, mufflers, connecting tubes, parallel paths, etc.) using instantaneous local mean values for the different variables. The domain is divided into fluid and solid CVs.

Momentum equation is characterized when the fluid refrigerant is flowing through a singularity (contract coefficient), or through a valve (effective force and flow area). Effective flow areas are evaluated considering multidimensional models based on modal analysis of fluid interaction in the valve. A staggered grid is employed to compute velocity field.

In order to evaluate the instantaneous compression chamber volume, force balances in the crankshaft connecting rod mechanical system are simultaneously solved at each time-step. The thermal analysis of the solid elements is based on global energy balances at each macro volume considered (shell, muffler, tubes, cylinder head, crankcase, motor, etc.).

The resulting governing equations (fluid flow, valve dynamics, conduction heat transfer in solids, etc.) are discretized by means of a fully implicit control volume formulation. The complete set of algebraic equations are coupled using the segregated pressure based algorithm Semi-Implicit Method for Pressure-Linked Equations (SIMPLEC) extended to compressible flow. The complete set of of discretized momentum, energy and pressure correction equations is solved by the direct method TDMA (Tri-Diagonal Matrix Algorithm).

Parallel circuits and extra elements (such us double orifices, resonators, etc.) are also considered in the formulation. The motor torque equation system is linearly independent, thus it is solved directly by means of inverse matrix system LU resolution. Instantaneous crank angle position is obtained from crank angle acceleration by means of the Heun method. Finally, macro-volumes energy balances are also directly solved by means of the inverse matrix system LU resolution. All theoretical basis of the numerical simulation model summarized above are described in detail in (Pérez-Segarra et al., 2003).

3.2 Compressor CL15 prototype

Table 3 presents an estimation of the main crankcase CL15 compressor prototype parameters: suction and discharge plenum, compression chamber characteristics and suction and discharge valve geometries.

Figure 5 shows the electrical motor experimental curves used in the CL15 compressor. The Figure details the motor torque, pulsation torque and electrical efficiency vs. instantaneous angular velocity of the motor considered.

Table 3: Crankcase compressor main parameters.

Inlet section diameter	6.2 mm	Outlet section diameter	5.0 mm
Suction line		Discharge line	
2 series chambers	5.08 cm^3	2 series chambers	9.0 cm^3
	1.65 cm^3		6.5 cm^3
plenum suction	1.00 cm^3	plenum discharge	6.6 cm^3
Shell volume	1596 cm^3	clereance ratio	4.38%
Compression chamber		Compression chamber	
bore diameter	14.0 mm	length stroke	9.744 mm
clearance volume	4.38 %	nominal frequency	3000 rpm
suction diameter (1)	3.2 mm	discharge diameter (2)	3.0 mm
suction stop	0.8 mm	discharge stop	0.8 mm
Suction valve geometry		Discharge valve geometry	
suction mass	0.712 g	discharge mass	1.071 g
suction ξ	3.51	discharge ξ	2.33
suction ω	5006.4 Hz	discharge ω	3340.6 Hz

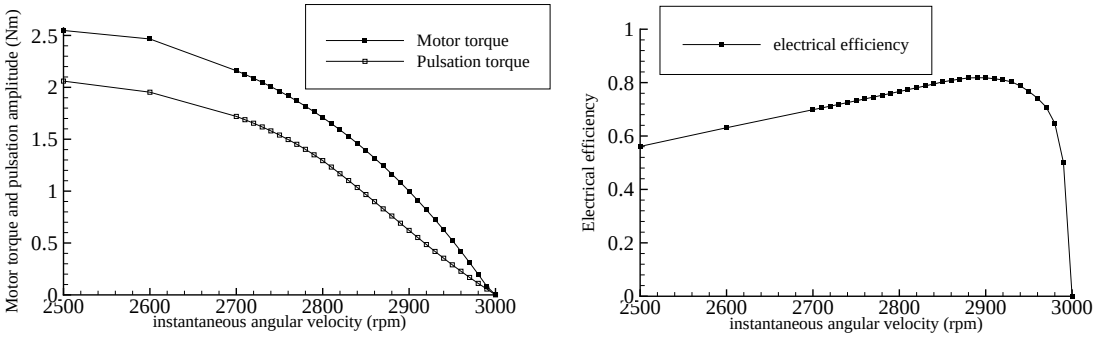

Figure 5: Experimental electrical motor values.

3.3 Comparative results

Table 4 shows the thermodynamic working conditions for both cycles studied, where p_{ev} and T_{ev} are the evaporation pressure and temperature, T_{sc} and p_c are the sub-cooling temperature and condensation pressure for the sub-critical cycle, while T_{gc} and p_{gc} are the gas cooler temperature and pressure respectively for the trans-critical cycle. T_{sh} shows the super-heating temperature and T_{amb} the ambient temperature.

Table 4: Thermodynamic working conditions for both studied cycles.

GLY80 sub-critical cycle							CL15 trans-critical cycle					
T_{ev}	p_{ev}	T_{sc}	p_c	T_c	T_{sh}	T_{amb}	T_{ev}	p_{ev}	T_{gc}	p_{gc}	T_{sh}	T_{amb}
T_4	p_4, p_1	T_3	p_3, p_2		T_1		T_1, T_2	p_1, p_2	T_3	p_3, p_2	T_1	
[^{o}C]	[bar]	[^{o}C]	[bar]	[^{o}C]	[^{o}C]	[^{o}C]	[^{o}C]	[bar]	[^{o}C]	[bar]	[^{o}C]	[^{o}C]
7.2	3.77	46	14.92	55.0	35.0	35.0	7.2	41.93	46	100.0	35.0	35.0

Tables 5 and 6 show the numerical comparative results under the conditions detailed above, where p_d corresponds to the condenser pressure or gas cooler pressure depending on sub-critical or trans-critical cycles respectively, $\dot{Q}_{ev}$ is the cooling capacity, T_{out} the outlet temperature, $\dot{m}$ the mass flow rate and η_v the volumetric efficiency. $\dot{W}_e$ corresponds to the power consumption, η_s is the isentropic efficiency, η_m and η_e are the mechanical and electrical efficiencies respectively, ω the mean frequency and COP the Coefficient of Performance.

Table 5: Numerical comparative results GLY80 vs. CL15.

$fluid$	p_{ev} [bar]	p_d [bar]	Π [-]	q_{ev} [kJ/kg]	$\dot{Q}_{ev}$ [kcal/h]	T_{out} [^{o}C]	$\dot{m}$ [kg/h]	$\dot{m}_l$ [kg/h]	η_v [%]
R134a	3.772	14.92	3.955	162.9	688.6	99.2	17.688	0.084	75.1
CO_2	41.93	100.0	2.385	196.7	793.1	128.6	16.868	1.901	67.8

Table 6: Numerical comparative results GLY80 vs. CL15.

$fluid$	w_{cp} [kJ/kg]	$\dot{W}_e$ [W]	η_s [%]	η_m [%]	η_e [%]	ω [Hz]	COP [-]
R134a	55.3	328.0	66.5	94.0	81.1	48.3	2.440
CO_2	63.4	394.3	65.0	93.9	80.1	48.2	2.338

The numerical results show that both compressors are able to obtain a similar cooling capacity, with an almost equal mass flow rates and close volumetric efficiencies. Mass flow rate differences are lower than 4.5%. It is interesting to remark that the main difference appears comparing the leakage between cylinder and piston. The CL15 compressor prototype has no piston rings. In the GLY80 the mass flow leakage is negligible, while in the CL15 the mass flow leakage is around 10% of the total mass flow rate.

The numerical results of both η_v show that GLY80 volumetric efficiency is 9.7% higher than CL15, while GL80 COP is around 4% higher than CL15. It is interesting to point out that the thermodynamic comparative analysis presented in section 1 predicts a trans-critical carbon dioxide COP very much lower than sub-critical R134a COP, while the numerical comparative study presented shows more similar COP. Thus, the ideal thermodynamic compressor behavior is far from the numerical model and real performance.

Figures 6 and 7 present a detailed evolution of the numerical comparative results depicted in the Tables presented above. Figure 6 shows the instantaneous frequency acceleration, motor torque and motor resistance, for both comparative compressor under periodical conditions. Figure 7 shows both pV diagrams, suction and discharge valve dynamics, together with the compression chamber pressure and temperature, the mass flow leakage and the instantaneous compression work.

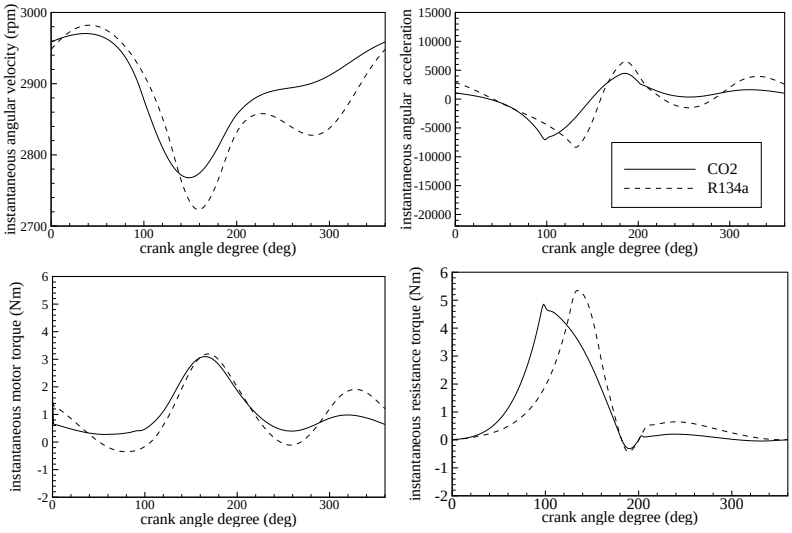

Figure 6: Instantaneous frequency, acceleration, motor torque and resistance.

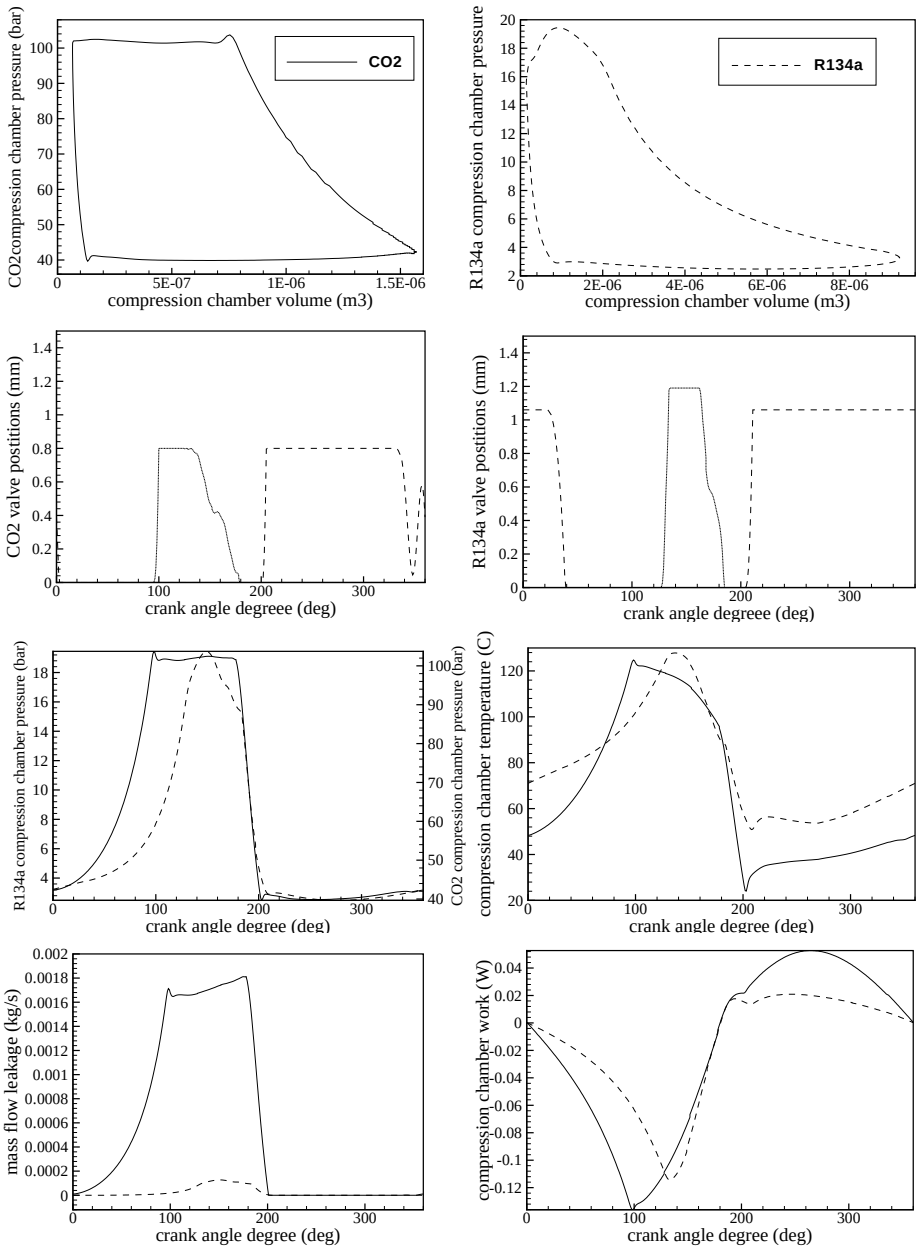

Figure 7: pV diagram, valve dynamics, compression chamber p and T evolution, mass flow leakage and cc work.

The valve dynamics evolution shows a very similar behavior in front of the fluid flow. Only the GLY80 suction valve opens longer, while discharge valve closes before than CL15 valve, due to the added spring valve. The instantaneous mass flow leakage is obviously much greater in the CL15 compressor than in the GLY80 compressor.

4. CONCLUSIONS

A thermodynamic comparative analysis between a conventional sub-critical R134a cycle and a trans-critical CO_2 cycle is presented in order to find an optimum CO_2 gas cooler pressure and to select the best working conditions.

A numerical comparative analysis between a commercial R134a compressor of 9.0cm^3 and a CO_2 compressor prototype of 1.5cm^3 is also shown in order to obtain similar working conditions. The numerical results presented clearly differs from the thermodynamic simplified analysis and demonstrate promising expectations and closer results comparing both compressors and cycles. The experimental investigation, the compressor prototype and CO_2 test results are presented in the companion paper.

REFERENCES

Fleming, J., 2003, Carbon dioxide as the working fluid in heating and/or cooling systems, *Bulletin of the International Institue of Refrigeration*, 83, no. 4:p. 7–15.

Jakobsen, A., 1998, Improving efficiency of trans-critical CO_2 refrigeration systems for reefers, *IIF-IIR comission D2/3*, Cambridge, UK, p. 130–138.

Kruse, H., Heidelck, R., and Süss, J., 1999, The application of CO_2 as a Refrigerant, *Bulletin of the International Institue of Refrigeration*, 79, no. 1:p. 2–21.

Liao, S., Zhao, T., and A., J., 2000, A correlation of optimal heat rejection pressures in transcritical carbon dioxide cycles, *Applied Thermal Engineering*, 20:p. 831–841.

Lorentzen, G., 1994, Revival of carbon dioxide as a refrigerant, *International Journal of Refrigeration*, 17, no. 5:p. 292–301.

Lorentzen, G. and Pettersen, J., 1993, A new, efficient and environmentally benign system for car air-conditioning, *International Journal of Refrigeration*, 16, no. 1:p. 4–12.

Pearson, A., 2001, New developments in industrial refrigeration, *ASHRAE J.*, 43, no. 3:p. 54–59.

Pérez-Segarra, C., Rigola, J., and Oliva, A., 2003, Modeling and numerical simulation of the thermal and fluid dynamic behavior of hermetic reciprocating compressors. Part 1: Theoretical basis., *International Journal of Heating, Ventilating, Air-Conditioning and Refrigerating Research*, 9, no. 2:p. 215 – 236.

Rigola, J., Pérez-Segarra, C., and Oliva, A., 2003, Modeling and numerical simulation of the thermal and fluid dynamic behavior of hermetic reciprocating compressors. Part 2: Experimental investigation., *International Journal of Heating, Ventilating, Air-Conditioning and Refrigerating Research*, 9, no. 2:p. 237 – 250.

Rigola, J., Raush, G., Pérez-Segarra, C., Oliva, A., Serra, J., Escribà, M., Pons, J., and Jover, J., 2004, Thermal and Fluid Dynamic Behavior of Trans-critical carbon dioxide Hermetic Reciprocating Compressors: Experimental Investigation., *International Compressor Engineering Conference*, Purdue University, IN, USA, in press.

Rozhentsev, A. and Wang, C., 2001, Some design features of a CO_2 air conditioner, *Applied Thermal Engineering*, 21:p. 871–880.

Taylor, C., 2002, Carbon dioxide-based refrigerating system, *ASHRAE J.*, 44, no. 9:p. 2–27.

(UNEP), 1987. United Nations Environmental Programme. Montreal Protocol on Substances that Deplete the Ozone Layer.

(UNFCCC), 1997. United Nations Framework Convention on Climate Change. Kyoto Protocol.

ACKNOWLEDGEMENTS

The authors gretefully acknowledge the financial support provided by CUBIGEL, S.A. - Unidad Hermética division of ACC Compressors (ref. no. C-04749), and by the Comisión Interministerial de Ciencia y Tecnología (ref. no. TIC2003-07970).